8296 *Macromolecules* **2010**, *43*, 8296–8303
DOI: 10.1021/ma101412r

Macromolecules
ARTICLE

Physical Aging in Ultrathin Polystyrene Films: Evidence of a Gradient in Dynamics at the Free Surface and Its Connection to the Glass Transition Temperature Reductions

Justin E. Pye, Kate A. Rohald, Elizabeth A. Baker, and Connie B. Roth*

Department of Physics, Emory University, Atlanta, Georgia 30322

Received June 24, 2010; Revised Manuscript Received September 1, 2010

ABSTRACT: We have measured the temperature dependence of the physical aging rate β of thick (2430 nm) and thin (29 nm) polystyrene (PS) films supported on silicon using a new streamlined ellipsometry procedure that we have recently developed. The physical aging rates $\beta(T)$ for the ~30 nm thick films are found to be reduced at all temperatures, which is not consistent with a simple shift in β corresponding to the average reduced glass transition temperature (T_g) of these films. Instead, the $\beta(T)$ results correspond well with there being a gradient in dynamics near the free surface. Our $\beta(T)$ results can be well fit by both a two-layer model and a gradient model. The temperature-dependent length scale (of order 10 nm) that characterizes the depth to which the enhanced dynamics near the free surface propagate into the film is similar to that found previously by Forrest and Mattsson [*Phys. Rev. E* **2000**, *61*, R53−R56] for the molecular weight (MW)-independent T_g reductions of low-MW free-standing PS films, strongly suggesting that the same mechanism is responsible for both effects. This length scale grows with decreasing temperature, suggesting that the mechanism is cooperative in nature.

Introduction

Numerous studies over the past nearly 20 years have reported deviations from bulk behavior in nanoconfined systems of the glass transition temperature (T_g) and associated properties such as physical aging, diffusion, and modulus.[1−15] Because of the growing number of technological applications that rely on the stability of glassy materials within domain sizes of tens to hundreds of nanometers, improved fundamental understanding of these phenomena is becoming critical. One important route to developing such an understanding is to determine how these various properties, which are interrelated in bulk systems, correlate in nanoconfined systems, if at all.

In recent years, a number of studies have investigated correlations between changes in physical aging rate, and time to reach equilibrium, with deviations of T_g in confined systems.[15−33] By definition, structural relaxation can only occur below T_g; thus, one would anticipate properties associated with physical aging to correlate with deviations in T_g. In some studies,[17,19−21,26,27] this has been found to be the case. However, most puzzling are studies, primarily from the gas permeation community, that indicate the length scale (film thickness) at which deviations in the physical aging rate occur can be much larger than the length scale at which deviations in T_g occur.[28−33] These results suggest that there are likely additional factors which influence the physical aging behavior beyond those that influence T_g in confined systems. Physical aging studies in confined systems have been recently reviewed by Priestley in ref 15; thus, we highlight here only those studies pertinent to our discussion. In the present study, we focus on changes in physical aging rates occurring near an interface on the length scale of tens of nanometers, which we believe are associated with corresponding changes in T_g. We have also observed changes in physical aging rates at much larger, hundreds of nanometers, length scale for films quenched in a free-standing state,[34] which will form the subject of a separate publication.

The majority of the investigations into the behavior of nanoconfined systems have focused on the glass transition. The deviations in T_g appear to be primarily associated with interfacial effects perturbing the dynamics rather than simply finite confinement of the material to nanometer-sized dimensions.[7,8,11,35−38] These interfacial effects are believed to lead to a gradient in dynamics emanating from the perturbing interface, with the material eventually returning to bulklike behavior sufficiently far from the interface. The observations that a free surface can impart enhanced dynamics or that hydrogen bonding at a substrate interface can reduce mobility are not particularly surprising. What seems to defy understanding is the strength and depth of the perturbation in dynamics. In some cases, shifts in T_g of many tens of degrees have been observed[1,2,11] with interfacial perturbations propagating up to tens to hundreds of nanometers from the interface.[8,15,38]

That a gradient in enhanced dynamics could exist near a free surface was originally proposed by Keddie, Jones, and Cory,[6] who developed an empirical fitting function, $T_g(h) = T_g^{bulk}[1 - (A/h)^\delta]$, for their T_g reductions in supported polystyrene (PS) films based on the idea of a liquidlike layer near the free surface. They assumed that the length scale characterizing the mobile free surface layer exhibited a power law divergence at bulk T_g with the reduced film $T_g(h)$ occurring when this length scale became equal to that of the film thickness h. Others have modeled this variation in dynamics with depth using various layer models,[39−42] with some proposing a different functional form for the thickness-dependent T_g reductions, $T_g(h) = T_g^{bulk}/(1 + h_0/h)$.[40,43−45] However, it was not until nearly a decade after the initial observations of T_g reductions in thin polymer films that Ellison and Torkelson[8] developed a unique fluorescence technique that could demonstrate experimentally that a gradient in T_g did exist near the free surface of PS. Surprisingly, these fluorescence multilayer measurements

*To whom correspondence should be addressed. E-mail: cbroth@emory.edu.

 Published on Web 09/17/2010

found that bulklike dynamics are not recovered until 30−40 nm from the interface,[8] a depth significantly larger than anticipated. Recent computer simulations by Baschnagel and co-workers[44,45] have also observed a gradient in dynamics near the free surface, and theoretical efforts by Lipson and Milner[46] have modified Long and Lequeux's percolation model[47] to model a variation in T_g with depth due to free surface and substrate interactions. What causes the enhanced dynamics at a free surface to propagate to depths of several tens of nanometers from the interface is perhaps the most complex unresolved issue associated with confinement.

Although a length scale of tens of nanometers in polymer systems immediately conjures ideas of chain size and radius of gyration (R_g), T_g reductions in supported PS films have been tested and found to be unequivocally independent of molecular weight (MW).[5,48−50] The same T_g reductions for a given film thickness h are observed for PS films with MWs both above and below the critical MW for entanglement and for R_g values comparable to and much less than the film thickness. What seems to influence the $T_g(h)$ behavior is the size and flexibility of the monomer unit and associated side group,[37,49−51] which suggests that cooperative segmental dynamics plays a role in this phenomenon. This cooperative motion idea is supported by a layer model analysis by Forrest and Mattsson[41,42] that fit their MW-independent $T_g(h)$ reductions for low-MW free-standing films using a layer model that allowed the thickness of the free-surface layer $\xi(T)$ with enhanced dynamics to vary with temperature in a manner similar to that anticipated for the size of the cooperatively rearranging region (CRR). A similar temperature dependence for the length scale quantifying the range of deviations in dynamics near the free surface was observed in computer simulations by Baschnagel and co-workers.[45] Studies have also demonstrated that T_g nanoconfinement effects can be reduced or completely eliminated by the addition of plasticizers,[52−54] which has been attributed to the plasticizer molecules reducing the cooperative nature of the dynamics.[52,53] However, careful studies by Torkelson and co-workers[49] and Vogt and co-workers[51] have yet to find a direct correspondence between T_g reductions in confined systems and the size of CRR.

Some physical aging studies have also found evidence for a gradient in dynamics occurring near a perturbing interface. Most notably, fluorescence multilayer measurements by Priestley, Torkelson, and co-workers[20] have shown a gradient in physical aging rate similar to that observed for T_g at both the free surface and substrate interface. However, their studies suggest that the length scale over which such perturbations propagate into the film may be larger than that observed for T_g changes.[20] Kawana and Jones[17] used ellipsometry to measure the overshoot of the expansivity−temperature curve (upon heating at 2 K/min) of ultrathin PS films that had been aged for 7 days at either 343 or 353 K. Studies of 10−200 nm thick films supported on silicon found no physical aging for 10 nm thick films that were aged below bulk T_g but above the reduced T_g of the film (consistent with observations made by fluorescence[19]). The authors interpreted the reduced intensity of the relaxation peak for thinner films as arising from the presence of a liquidlike layer at the free surface of order 10 nm, but they hypothesized that local structural relaxation would be depth dependent reflecting the gradient in T_g present in these films. Recent studies by Rowe et al.[26,27] have observed correlations between physical aging measured using gas permeation and T_g reductions for ultrathin polysulfone (PSF) films and found that the sizes of free volume elements were different in the near surface region than in the interior of the film. In contrast, Koh and Simon,[21] who have used differential scanning calorimetry (DSC) to measure the enthalpy overshoots of stacked PS films for aging times out to 1000 min at temperatures down to $T_g - 15$ K, found that the physical aging rate of PS films at a fixed aging temperature decreased with decreasing film thickness and that this decrease was consistent with a simple shift in the temperature dependence of the physical aging rate caused by a shift in T_g. The authors also investigated the time to reach equilibrium at a few degrees below T_g and found that thinner films reach equilibrium more quickly.

In the present study, we have used a newly developed streamlined ellipsometry technique[55] to measure the temperature dependence of the physical aging rate of ultrathin supported PS films. The physical aging rate is determined from time-dependent measurements of the film thickness quantifying the increase in average film density during aging. A comparison of the temperature dependence of the aging rate between thick (2430 nm) and thin (29 nm) films reveals that the aging rates for the thinner films are not simply shifted to lower temperatures corresponding to the shift in the average T_g of these films, but that the physical aging rates are reduced at nearly all aging temperatures for PS films < 100 nm thick. We find these results to be consistent with a gradient in dynamics present at the free surface, i.e., that the rate of structural relaxation varies with distance from the free surface. The temperature dependence of the reduced physical aging rates has been analyzed using a popular two-layer model, from which we extract a temperature-dependent liquidlike layer at the free surface (of order 10 nm) that characterizes the depth dependence of the gradient in dynamics. We find the temperature dependence of this length scale to be very similar to that previously found to describe the film thickness-dependent T_g reductions in these films, strongly suggesting that the enhanced dynamics at the free surface are responsible for both effects. In addition, we have analyzed our data in terms of a more realistic continuous distribution (gradient) in dynamics. In both the two-layer model and gradient model, we observe that the length scale that describes the depth to which the enhanced dynamics at the free surface propagate into the film grows with decreasing temperature, bringing renewed support to the idea that the mechanism controlling this behavior involves cooperative motion of the segmental units.

Experimental Section

Polystyrene (Sigma-Aldrich secondary standard) with M_w = 245 000 g/mol, M_w/M_n = 2.0, as determined by GPC relative to PS standards,[55] was dissolved in toluene at concentrations from 1 to 15 wt %. PS films with thicknesses from 29 to 2700 nm were formed by spin-coating at 500−3000 rpm onto silicon substrates (∼500 μm thick) that were precut into 2 cm square pieces. All supported PS films were subsequently annealed under vacuum at 393 K for at least 12 h to remove residual solvent and ensure a uniform sample history. Some of the thickest films (∼2500 nm) were annealed under vacuum for up to 48 h, but these films produced identical experimental results to those obtained with films annealed for only 12 h. No evidence of dewetting was observed after annealing for any of the thick or thin PS films. The glass transition temperature for the PS used was 374 K as measured by DSC (T_g onset at 10 K/min on second heat after cooling at 20 K/min)[55] and 370 ± 2 K as measured by ellipsometry (T_g from film thickness on cooling at 1 K/min) based on an average of five samples ∼2500 nm in thickness.

At the start of each physical aging measurement, the PS films supported on silicon were annealed in a glass Petri dish above T_g at 403 K for 25−30 min to equilibrate the sample and erase all previous thermal history. The films were thermally quenched by removing them from the oven and placing the glass Petri dish in thermal contact with a room temperature aluminum block for 60 s. This ensured a rapid (∼100 K/min), reproducible temperature quench of the sample through T_g. The sample was then immediately transferred to the ellipsometer hot stage (Instec heater) that was preset and stabilized (for ∼30 min) at the desired aging temperature. The sample was quickly aligned on the ellipsometer (Woollam M-2000) and data collection initiated. Continuous

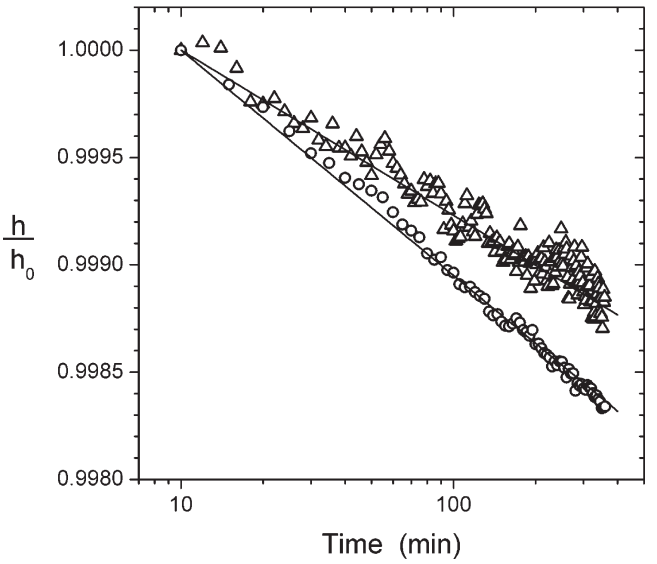

Figure 1. Film thickness h, normalized by h_0, the film thickness corresponding to an aging time of 10 min when the sample is ensured to be in thermal equilibrium with the aging temperature of 338 K, as a function of the logarithm of the aging time. Circles are data from a 2300 nm thick PS film with the best fit line corresponding to an aging rate $\beta = 10.5 \times 10^{-4}$, and the triangles are data from a 29 nm thick PS film with a best fit aging rate of $\beta = 7.7 \times 10^{-4}$. The physical aging rates were evaluated using $\beta = -1/h_0\ dh/d(\log t)$.

measurements of the ellipsometric angles Ψ and Δ as a function of wavelength λ at an angle of incidence of 65° were collected (averaging over a 30 s period) every 2 min for 360 min. The film thickness h and index of refraction $n(\lambda)$ of the polymer film were determined by fitting the $\Psi(\lambda)$ and $\Delta(\lambda)$ values for $\lambda = 400-1000$ nm to a layer model comprised of the polymer film, modeled as a Cauchy layer with $n(\lambda) = A + B/\lambda^2 + C/\lambda^4$, atop a silicon substrate with a 2 nm native oxide layer.

Results and Discussion

Physical aging rates β were calculated by plotting the normalized film thickness h/h_0 as a function of the logarithm of the aging time, as depicted in Figure 1. The value of h_0 corresponds to the thickness at an aging time of 10 min, when it is ensured that the sample has reached thermal equilibrium with the aging temperature. The slope of the linear decrease in film thickness as a function of the logarithm of the aging time characteristic of physical aging is evaluated by a single parameter fit with the data forced to pass through the first data point corresponding to an aging time of 10 min:[55]

$$\beta = -1/h_0\ dh/d(\log t) \quad (1)$$

Figure 1 shows data for a 2300 nm thick film with $\beta = 10.5 \times 10^{-4}$ and a 29 nm thick film with $\beta = 7.7 \times 10^{-4}$ aged at 338 K for 360 min. We have previously explored the use of different aging times and found that the physical aging rates obtained from data collected for 360 min are within experimental error of those obtained from data collected for 24 h of aging.[55]

Figure 2 examines the effect of film thickness on the physical aging rate of PS films supported on silicon. In this figure, all of the data have been collected at an aging temperature of 338 K, corresponding to the peak in the temperature dependence of our measured aging rate for ~2500 nm thick films (plotted in Figure 3). Using ellipsometry, the thickest films we are able to reliably measure are ~2500 nm. For thicknesses beyond this, the oscillations in the Ψ and Δ data as a function of wavelength, and the difficulty associated with producing optically flat samples,

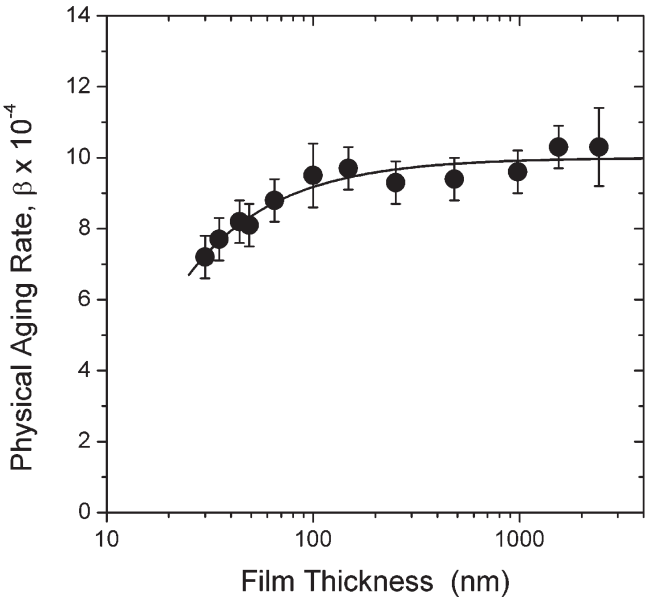

Figure 2. Physical aging rate β plotted as a function of film thickness for PS films supported on silicon for data collected at an aging temperature of 338 K over a period of 360 min. Each data point corresponds to an average of 2−6 samples. The curve is a best fit to $\beta(h) = \beta_{bulk}(1 - A/h)$ with $\beta_{bulk} = 10 \times 10^{-4}$ and $A = 8 \pm 1$ nm for this aging temperature.

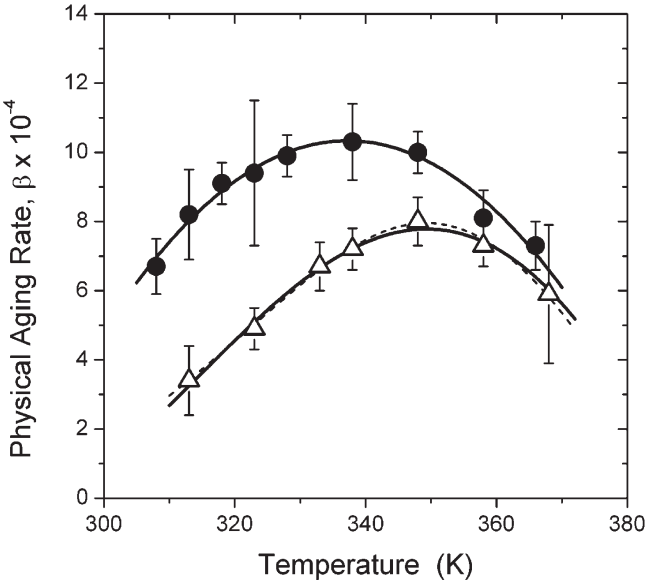

Figure 3. Temperature dependence of the physical aging rate β plotted for 2430 ± 120 nm thick PS films (filled circles) and for 29 ± 1 nm thick PS films (open triangles). Each data point corresponds to an average of 2−6 samples measured over an aging period of 360 min evaluated using $\beta = -1/h_0\ dh/d(\log t)$. The curve through the ~2500 nm thick PS films is simply a second-order polynomial fit to parametrize the temperature dependence of the data, $\beta_{bulk}(T)$. The solid curve through the ~30 nm thick PS films is for eq 2 with $A(T)$ given by the best fit of eq 3 to the data shown in Figure 4, while the dotted curve is for eq 5 with $\lambda(T)$ given by the best fit of eq 3 to the data shown in Figure 4.

degrade the fit to the layer model. The thinnest films we can reliably measure are ~30 nm. At this thickness the total change in film thickness over the entire 360 min aging run is < 0.1 nm (~0.3% change in film thickness). We recognize this change in thickness with aging time is exceedingly small and that one might question the reliability of such a measurement. However, each data point shown in Figure 2 is an average of multiple measurements

over 2−6 samples (more for the thinner films). In addition, we have performed control experiments on 30 nm thick films held above T_g in the equilibrium state and find that the measured film thickness is stable to within 0.011 nm over the course of the 360 min measurement, corresponding to a change in overall film thickness of $<0.04\%$. Below ~30 nm, the difficulties associated with the inability of ellipsometry to independently resolve[56,57] h and n make the aging measurement problematic.

The data shown in Figure 2 indicate that for PS film thicknesses ≥100 nm the measured aging rate is independent of film thickness, while for films <100 nm in thickness we see a progressive decrease in the physical aging rate. Because of the well-known reductions in T_g with decreasing film thickness that have been abundantly characterized for PS films supported on silicon for thicknesses less than ~100 nm,[2,5] our initial interpretation of the data shown in Figure 2 was that a shift in the temperature dependence of the aging rate to lower temperatures had occurred, corresponding to the shift in T_g. In other words, the decrease in the aging rate for films with thicknesses <100 nm was associated with the peak in the aging rate no longer corresponding to 338 K. This would be consistent with recent observations in the research literature which used DSC to measure stacked PS films for aging temperatures down to $T_g - 15$ K[21] and with those studies that have measured no physical aging for ultrathin PS films at aging temperatures below bulk T_g but above the reduced T_g of the film.[17,19]

To test this assumption, we measured the temperature dependence of the physical aging rate for 29 ± 1 nm thick PS films supported on silicon. Figure 3 compares the temperature dependence of the physical aging rate for 2430 ± 120 nm and 29 ± 1 nm thick PS films, both collected over an aging period of 360 min with β evaluated using eq 1. It is clear from the data that the physical aging rate for the thinner films is generally reduced at all temperatures and has not simply shifted to lower temperatures as anticipated by the reduced average T_g of these films. The reduced physical aging rates imply that the percentage decrease in film thickness during the 360 min aging process is less for the thinner films.

On first consideration, it may appear that the results presented in Figures 2 and 3 are not consistent with the fluorescence measurements by Priestley et al., which found no change in the physical aging rate between 500 and 20 nm thick PS films supported on silica measured over an aging period of 80 min at 305 K.[19] However, the pyrene fluorescence studies by Ellison and Torkelson,[8] which demonstrated the T_g gradient in PS films as a function of depth from the free surface, also found that films thinner than 25 nm can no longer support a gradient in the T_g dynamics. Thus, significant differences in the film dynamics may exist between 20 and 30 nm thick films. Unfortunately, we are unable to reliably measure films less than ~30 nm with ellipsometry.

Numerous studies presented in the research literature have demonstrated that the *average* T_g of 30 nm thick PS films are reduced from the bulk value by 5−10 K.[2,5] It is clear that the results of Figure 3 are *not* consistent with the thinner films having simply a single T_g value reduced from the bulk, since that would be observed as a simple shift in the temperature dependence of the bulk aging rate in Figure 3 to lower temperatures by 5−10 K. What is most peculiar is that we observe physical aging of 29 ± 1 nm thick PS films at an aging temperature of 368 K, only a few degrees below bulk T_g. This indicates that some portion of the ~30 nm thick films must be in the glassy state, which would be consistent with these films having a gradient in T_g dynamics across the thickness of the film, as has been measured experimentally using fluorescence.[8] The large error bar associated with this data point arises from the small variation in film thickness between the measured films. At an aging temperature of 368 K, very close to bulk T_g, the measured aging rate is very sensitive to film thickness. The five films measured at 368 K that gave an average aging rate of $(5.9 \pm 2.0) \times 10^{-4}$ are 30.0 nm with $\beta = 8.2 \times 10^{-4}$, 29.0 nm with $\beta = 5.9 \times 10^{-4}$, 28.3 nm with $\beta = 7.2 \times 10^{-4}$, 28.2 nm with $\beta = 5.2 \times 10^{-4}$, and 27.3 nm with $\beta = 2.9 \times 10^{-4}$.

We now demonstrate that the results of Figures 2 and 3 are consistent with a gradient in T_g dynamics across the thickness of the film. One can envision modeling a gradient in T_g dynamics by dividing a 30 nm thick film into six layers of 5 nm each, with each layer exhibiting its own T_g and aging rate β. The bottommost layer next to the substrate interface would exhibit nearly bulklike properties,[8] while the topmost layer next to the free surface would exhibit nearly liquidlike properties.[8,20] It is reasonable to assume that the region of the film immediately next to the free surface does not undergo any physical aging because its local T_g, much reduced from the average film T_g, would be lower than the aging temperature. However, ellipsometry is only able to measure a single average β value across the entire thickness of the film. Thus, with a single measured parameter, the most sophisticated layer-type model we are able to interpret is a simple two-layer model with a liquidlike layer at the free surface that does not undergo any physical aging at the aging temperature and a bulklike aging layer underneath. Such a two-layer model gives rise to a simple parametrization for the data:

$$\beta(h, T) = \beta_{bulk}(T)[1 - A(T)/h] \quad (2)$$

where our single measured parameter can be used to comment on the liquidlike layer thickness $A(T)$ that characterizes the depth from the free surface that the enhanced mobility persists. Numerous other studies with similar limitations have interpreted their data in this manner, obtaining a liquidlike layer thickness of 5−10 nm at the free surface of PS.[6,17,41,42] However, all these studies have also remarked that although the analysis is performed with a simple two-layer model, it is far more likely that the change in dynamics across the thickness of the film occurs uniformly as a gradient in dynamics as a function of depth.[8,20,44] This point should not be forgotten.

A fit of eq 2 to the $\beta(h)$ data presented in Figure 2 at an aging temperature of 338 K gives best fit values of $\beta_{bulk} = 10 \times 10^{-4}$ and a liquidlike layer thickness of $A = 8 \pm 1$ nm, which is independent of the overall film thickness. The data in Figure 2 are well fit by the simple two-layer model and provide a liquidlike layer thickness consistent with previous work.[6,17,41,42] To determine whether this analysis is consistent with the physical aging rates measured over the range of temperatures shown in Figure 3, we parametrize the $\beta_{bulk}(T)$ data in Figure 3 by fitting the 2430 ± 120 nm thick films to a second-order polynomial and use it to extract $A(T)$ values from the $\beta(T)$ data for the 29 ± 1 nm thick films shown via eq 2. This surface layer thickness $A(T)$ is plotted in Figure 4.

From the $A(T)$ data plotted in Figure 4, it is immediately apparent that the effective surface layer thickness increases with decreasing temperature, starting from ~3 nm just below bulk T_g. This may initially appear counterintuitive but has been previously observed by Forrest and Mattsson,[41,42] who performed a similar layer-model analysis of their $T_g(h)$ data for free-standing low-molecular-weight PS films. We note that the *low*-MW free-standing film data exhibit the same functional form for $T_g(h)$ as supported films with no MW dependence, the only difference being that for free-standing films the T_g reduction for a given film thickness h is twice as large as for a supported film of thickness h because of the presence of two free surfaces.[1,2,41,42] This is in contrast to the $T_g(h)$ data for *high*-MW free-standing films which exhibit a qualitatively different behavior with a strong MW dependence.[1,2] For comparison, we include dashed and dotted lines in Figure 4 depicting the range of the calculated values by

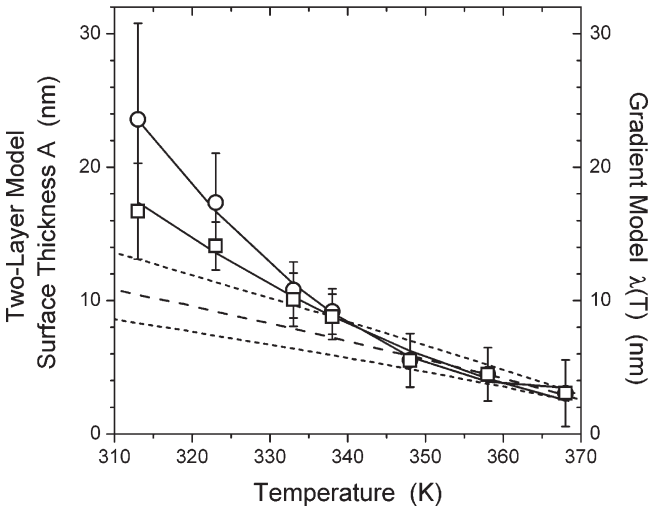

Figure 4. Squares correspond to the temperature dependence of the surface layer thickness $A(T)$ for the two-layer model, determined using eq 2 from the $\beta(T)$ data for the ~30 nm thick PS films, while the solid curve is a best fit of eq 3 to the data. The dashed and dotted curves represent the range of surface layer thickness $A(T)$ values obtained by Forrest and Mattsson[41,42] using a similar two-layer model analysis from T_g measurements on low-MW free-standing PS films. Circles correspond to the temperature dependence of the characteristic length $\lambda(T)$ for the gradient model, determined using eq 5 from the $\beta(T)$ data for the ~30 nm thick PS films, while the solid curve is a best fit of eq 3 to the data. See text for details of the best fit parameter values.

Forrest and Mattson[41,42] for the surface layer thickness. Given that their values were obtained from T_g measurements on free-standing PS films using Brillouin light scattering[42] and ours were obtained from physical aging measurements on supported PS films using ellipsometry, the agreement is quite remarkable. The similarity also strongly suggests that our reduced physical aging rates observed for PS films < 100 nm thick are related to the T_g reductions observed in these films.

How should this growing surface layer thickness $A(T)$ with decreasing temperature be interpreted? $A(T)$ represents, in some (unfortunately) ill-defined manner, the depth to which the enhanced free-surface mobility propagates into the film. Recent computer simulations by Baschnagel and co-workers[44,45] have observed that the length scale over which the enhanced dynamics at the free surface transition continuously into bulklike dynamics increases with decreasing temperature, consistent with this observation. Forrest and Mattsson[41,42] related the temperature dependence of the surface layer thickness to the temperature dependence of the cooperativity length $\xi(T)$, suggesting that the propagation of enhanced mobility from the free surface may be correlated with cooperative motion. Although this is an appealing idea, it is not clear that T_g nanoconfinement effects correlate directly with the cooperativity length scale.[49−51]

Following Forrest and Mattsson,[41] we fit the temperature dependence of our surface layer thickness $A(T)$ to a functional form for $\xi(T)$ proposed by Donth and co-workers:[58−60]

$$A(T) = \xi(T) = r_0 + \alpha(T_{ons} - T)^{\gamma} \qquad (3)$$

The characteristic length $\xi(T)$ grows with decreasing temperature starting from an onset temperature for cooperative motion T_{ons} (in the vicinity of the $\alpha\beta$ splitting region), with a minimum $\xi(T_{ons})$ size of r_0 assumed to be one monomer diameter[60] (for PS, Forrest and Mattsson[41] took $r_0 = 0.6$ nm). For bulk PS, T_{ons} is estimated[41,42,58,59] to be 463 ± 15 K, ~90 K above T_g. The power-law dependence of $\xi(T)$ is characterized by two fitting parameters α and γ.[61] Forrest and Mattsson[41] obtained best fit values of $\gamma = 2.0 \pm 0.1$, $\alpha = (2.95 \pm 0.30) \times 10^{-3}$, and $T_{ons} = 485 \pm 6$ K, holding r_0 fixed at 0.6 nm. Using the temperature dependence of eq 3 for their free surface layer, Forrest and Mattsson also obtained an effective T_g for their surface layer by fitting their average film $T_g(h)$ data for low-MW free-standing films to a three-layer model comprised of two outer layers of thickness $\xi(T)$ with T_g^{surf} and an inner layer of thickness $h - 2\xi(T)$ with T_g^{bulk} (see Figure 6 of ref 42) giving a value of $T_g^{surf} = 300 \pm 7$ K.[41] We have fit eq 3 to our $A(T)$ data presented in Figure 4 with r_0 and γ fixed[62] at the values obtained by Forrest and Mattsson,[41] $r_0 = 0.6$ nm and $\gamma = 2$, obtaining best fit values of $\alpha = (2.4 \pm 1.0) \times 10^{-3}$ and $T_{ons} = 396 \pm 13$ K. If we assume that T_g occurs ~90 K below the onset of cooperative motion T_{ons}, then this would suggest a T_g for our surface layer of $T_g^{surf} \approx 306$ K, in the same temperature range previously estimated by Forrest and co-workers.[41,42] Although this agreement with previous estimates of a surface T_g is intriguing, we hesitate to attach undue weight to this particular form of eq 3, as the $A(T)$ data could be equally well described by other functional forms. Several functional forms for the temperature dependence of the cooperative length scale $\xi(T)$ have been proposed, as described in refs 63 and 64. We should note that Forrest and co-workers[65] have also recently applied this similar type of analysis to nanoparticle embedding measurements and obtained reasonable agreement with the results presented in Figure 4.

To demonstrate that this temperature dependence of $A(T)$ describes the observed $\beta(T)$ values for the ~30 nm thick PS films, we include in Figure 3 the curve corresponding to $\beta(T)$ from eq 2 with $A(T)$ given by eq 3. This analysis demonstrates that the temperature dependence of the physical aging rate for the $h \approx 30$ nm thick PS films shown in Figure 3 is consistent with the presence of a gradient in dynamics as a function of depth from the free surface. In addition, this analysis indicates that the depth to which the enhanced dynamics penetrate into the film from the free surface increases with decreasing temperature, suggesting that the mechanism for the propagation of enhanced dynamics from the interface is related to cooperative motion.

Alternatively, we can fit our data to a more realistic gradient-type model that more accurately represents the continuous change in dynamics with depth. A reasonable (simplest) approach would be to assume a single-exponential decay of the aging rate from zero at the free surface to its bulk value, $\beta_{bulk}(T)$, at a depth z sufficiently far from the free surface:

$$\beta(z,T) = \beta_{bulk}(T)[1 - \exp(-z/\lambda(T))] \qquad (4)$$

This would define a characteristic length scale $\lambda(T)$ that would describe the depth to which the enhanced dynamics at the free surface propagate into the film. We believe that such a definition of $\lambda(T)$ has a more well-defined meaning than the $A(T)$ parameter describing a "liquidlike" layer size of the somewhat artificial two-layer model. The general functional form of eq 4 is supported by the fluorescence multilayer measurements of Priestley et al.[20] and by a more recent observation indicating that no physical aging occurs at a free surface.[66] We note that there is a much more solid basis in the literature for a gradient in T_g with depth. While we have already shown that a simple shift of the temperature dependence of the *average* physical aging rate $\beta(h,T)$ to lower temperatures corresponding to the *average* reduced $T_g(h)$ for thin films does not occur, a similar shift may occur for the *local* aging rate $\beta(z,T)$ at a given depth z due to the reduced *local* T_g at that depth $T_g(z)$.

From eq 4, we define the average, experimentally measured, film thickness-dependent aging rate as the arithmetic mean:

$$\beta(h,T) = \frac{1}{h}\int_0^h \beta(z,T)\,dz$$

$$= \beta_{bulk}(T)\left[1 - \frac{\lambda(T)}{h}\left\{1 - \exp\left(-\frac{h}{\lambda(T)}\right)\right\}\right] \qquad (5)$$

Lipson and Milner[46] have recently discussed whether or not such a "democratic" average, versus perhaps a weighted average, is the most appropriate. Baschnagel and co-workers[44] have also remarked that even though the average $T_g(h)$ of the film may be a simple arithmetic mean, this does not imply that other quantities, such as the average relaxation time of the film, are also a simple average of the local depth-dependent values. However, without a specific reason to try something more complicated, we proceed here with the simplest definition. Nevertheless, it is worth keeping in mind that different experimental techniques may average across the distribution in dynamics in a different manner.[12]

The $\lambda(T)$ data shown in Figure 4 were obtained from the $\beta(T)$ data for the 29 ± 1 nm thick films via eq 5 in a manner similar to how the $A(T)$ data were obtained from eq 2. In Figure 4, the $\lambda(T)$ data are fit to $\lambda(T) = \xi(T)$ given by eq 3,[67] and the dashed curve in Figure 3 corresponds to $\beta(h = 30 \text{ nm}, T)$ for the $\lambda(T)$ data. It is worth noting that eq 5, the $\beta(h,T)$ for the gradient model, reduces to eq 2, the $\beta(h,T)$ for the two-layer model, when the film thickness is large (i.e., $h \gg \lambda$). This explains why the $\lambda(T)$ and $A(T)$ values overlap for the higher aging temperatures (see Figure 4) when $\lambda(T) < \sim 10$ nm, sufficiently less than the $h \approx 30$ nm film thickness. Both $\lambda(T)$ and $A(T)$ are of order 10 nm and increase with decreasing temperature. These two parameters are not significantly different but simply illustrate two different methods of characterizing the depth to which the enhanced dynamics at the free surface propagate into the film.

We recognize that changes in T_g or α-relaxation dynamics are not always observed with decreasing film thickness.[9,68−74] Many of these factors have been addressed. For instance, studies addressing issues associated with sample preparation and residual stresses from spin-coating have found that local chain conformations can be sufficiently relaxed after annealing times of ∼20 min at $T_g^{bulk} + 20$ K.[75−78] This indicates that overall global chain conformations do not affect T_g[7,79] yet would probably influence other dynamics such as viscosity and dewetting. Confinement effects tend not to be observed at temperatures above bulk T_g[79] or when measurements are carried out at high frequencies.[80] Unintended water uptake in some polymers can act as a plasticizer also eliminating confinement effects.[54] Confinement effects in supported polymer films generally result in a broadening of the T_g dynamics combined with a loss in contrast of the transition.[81] This can explain much of the variability observed in the literature as different experimental techniques are sensitive to different parts of the glass transition.[2,12,82] Experimental measurements of ultrathin films are technically challenging because little material is available to provide a signal. In addition, the strength of free surface effect can be much weaker in some polymers.[11,37,83] For example, the impact of interfacial interactions can vary with tacticity[84] or small differences in monomer structure,[37] such that competing effects between the free surface and substrate interface can cancel out, resulting in little or no change in T_g with decreasing film thickness. Overall, these studies provide intriguing insight into what factors control glass transition dynamics in confined systems and suggest methods by which confinement effects may be controlled in order to tune material properties.

Here we have demonstrated for the first time that the temperature-dependent length scale characterizing the depth to which enhanced dynamics are propagated from the free surface of PS is the same for both reductions in the physical aging rate and reductions in T_g, strongly suggesting that both effects are caused by the same mechanism. This mechanism appears to be responsible for both the MW-independent $T_g(h)$ reductions observed in supported PS films[2,6,8,48,49] and the MW-independent $T_g(h)$ reductions of *low*-MW free-standing PS films,[1,41,42] which are both qualitatively similar, following the Keddie, Jones, and Cory[6] functional form. (This is in contrast to *high*-MW free-standing films which exhibit a qualitatively different $T_g(h)$ behavior with a strong MW dependence.[1,2]) This MW-independent mechanism manifests as a gradient in enhanced dynamics near a free surface that propagates into the film for some distance before bulklike dynamics are recovered. We have observed that the length scale characterizing this gradient in dynamics grows with decreasing temperature, bringing renewed support to the idea that the mechanism that propagates the enhanced dynamics from the free surface is related to cooperative motion of the segmental units.

The fact that the length scale of the effect grows with decreasing temperature may explain some discrepancies in the research literature pertaining to the size of the near surface region that exhibits enhanced dynamics. For instance, studies of surface mobilities at elevated temperatures near bulk T_g or when more liquidlike properties are probed tend to observe enhanced dynamics to a depth of only a few nanometers.[65,85] In contrast, fluorescence multilayer measurements by Torkelson and coworkers have indicated that bulklike dynamics are not recovered until depths of 30−40 nm from the free surface of PS.[8] Both of these results are consistent with our observations. As shown in Figure 4, the characteristic length describing the depth to which the enhanced dynamics propagate from the free surface is only a few nanometers near bulk T_g but grows to approximately 15−20 nm for temperatures 50−60 °C below bulk T_g. At the temperatures at which the Torkelson fluorescence measurements observe a reduced T_g of the PS surface,[8] $T_g^{bulk} - 32 \text{ K} \approx 340$ K, our characteristic length $\lambda(T)$ for the exponential decay of the enhanced dynamics near the free surface is ∼8 nm. For a single-exponential decay that forms the basis of eq 4, four to five characteristic length λ's, i.e., 32−40 nm, would be necessary before the dynamics would appear bulklike (to within experimental error). However, we note that these results do not agree with the extremely large length scale effects observed by the gas permeation community[28−33] that find differences in physical aging rates for film thicknesses of several micrometers. Because no corresponding T_g changes are observed at micrometer length scales, this suggests that other unrelated effects may be the cause of those results. This remains unexplained and worth further study. Another open question is whether or not confined systems age to the same equilibrium state as that of bulk. It is clear that the rate at which structural relaxation occurs in confined geometries is frequently different and does not necessarily correlate with T_g changes,[86] but there is also evidence[16] that when equilibrium can be reached, it is not the same equilibrium state as that of bulk.

Conclusions

Using ellipsometry, we have measured the temperature dependence of the physical aging rate for thick (2430 nm) and ultrathin (29 nm) PS films supported on silicon. We find that the thinner films have reduced physical aging rates at nearly all temperatures, a result that does not correspond simply to the shift in the average T_g of these films. The reduced physical aging rates of these films are consistent with a depth-dependent gradient in dynamics that is approximated by a two-layer model with a nearly liquidlike surface layer of order 10 nm. The thickness of the surface layer, which characterizes the depth to which the enhanced mobility at the free surface penetrates into the film, grows with decreasing temperature, suggesting that the mechanism for the propagation of enhanced dynamics from the interface is related to cooperative motion. Our physical aging measurements using ellipsometry on ultrathin supported PS films can be explained with an analysis similar to that used by Forrest and Mattsson[41,42] for T_g measurements using Brillouin light scattering of low-MW free-standing PS films, strongly suggesting that the reduced physical aging rates observed in PS films < 100 nm thick are related to the T_g

reductions observed in these films. We also present an analysis in terms of a gradient model that more realistically characterizes the continuous distribution in dynamics believed to exist at the free surface of these films.

Acknowledgment. We acknowledge support from the Petroleum Research Fund (Grant PRF-48927-DN17, CBR) and Emory University.

References and Notes

(1) Forrest, J. A.; Dalnoki-Veress, K. *Adv. Colloid Interface Sci.* **2001**, *94*, 167–196.
(2) Roth, C. B.; Dutcher, J. R. *J. Electroanal. Chem.* **2005**, *584*, 13–22.
(3) Baschnagel, J.; Varnik, F. *J. Phys.: Condens. Matter* **2005**, *17*, R851–R953.
(4) Alcoutlabi, M.; McKenna, G. B. *J. Phys.: Condens. Matter* **2005**, *17*, R461–R524.
(5) Tsui, O. K. C. In *Polymer Thin Films*; Tsui, O. K. C., Russell, T. P., Eds.; World Scientific: Singapore, 2008; pp 267−294.
(6) Keddie, J. L.; Jones, R. A. L.; Cory, R. A. *Europhys. Lett.* **1994**, *27*, 59–64.
(7) Sharp, J. S.; Forrest, J. A. *Phys. Rev. Lett.* **2003**, *91*, 235701.
(8) Ellison, C. J.; Torkelson, J. M. *Nature Mater.* **2003**, *2*, 695–700.
(9) O'Connell, P. A.; McKenna, G. B. *Science* **2005**, *307*, 1760–1763.
(10) Stafford, C. M.; Vogt, B. D.; Harrison, C.; Julthongpiput, D.; Huang, R. *Macromolecules* **2006**, *39*, 5095–5099.
(11) Roth, C. B.; McNerny, K. L.; Jager, W. F.; Torkelson, J. M. *Macromolecules* **2007**, *40*, 2568–2574.
(12) Kim, S.; Hewlett, S. A.; Roth, C. B.; Torkelson, J. M. *Eur. Phys. J. E* **2009**, *30*, 83–92.
(13) Kim, C.; Facchetti, A.; Marks, T. J. *Science* **2007**, *318*, 76–80.
(14) Swallen, S. F.; Kearns, K. L.; Mapes, M. K.; Kim, Y. S.; McMahon, R. J.; Ediger, M. D.; Wu, T.; Yu, L.; Satija, S. *Science* **2007**, *315*, 353–356.
(15) Priestley, R. D. *Soft Matter* **2009**, *5*, 919–926.
(16) Simon, S. L.; Park, J. Y.; McKenna, G. B. *Eur. Phys. J. E* **2002**, *8*, 209–216.
(17) Kawana, S.; Jones, R. A. L. *Eur. Phys. J. E* **2003**, *10*, 223–230.
(18) Ellison, C. J.; Kim, S. D.; Hall, D. B.; Torkelson, J. M. *Eur. Phys. J. E* **2002**, *8*, 155–166.
(19) Priestley, R. D.; Broadbelt, L. J.; Torkelson, J. M. *Macromolecules* **2005**, *38*, 654–657.
(20) Priestley, R. D.; Ellison, C. J.; Broadbelt, L. J.; Torkelson, J. M. *Science* **2005**, *309*, 456–459.
(21) Koh, Y. P.; Simon, S. L. *J. Polym. Sci., Part B: Polym. Phys.* **2008**, *46*, 2741–2753.
(22) Cangialosi, D.; Wubbenhorst, M.; Groenewold, J.; Mendes, E.; Schut, H.; van Veen, A.; Picken, S. J. *Phys. Rev. B* **2004**, *70*, 224213.
(23) Cangialosi, D.; Wubbenhorst, M.; Groenewold, J.; Mendes, E.; Picken, S. J. *J. Non-Cryst. Solids* **2005**, *351*, 2605–2610.
(24) Fukao, K.; Sakamoto, A. *Phys. Rev. E* **2005**, *71*, 041803.
(25) Fukao, K.; Koizumi, H. *Phys. Rev. E* **2008**, *77*, 021503.
(26) Rowe, B. W.; Freeman, B. D.; Paul, D. R. *Polymer* **2009**, *50*, 5565–5575.
(27) Rowe, B. W.; Pas, S. J.; Hill, A. J.; Suzuki, R.; Freeman, B. D.; Paul, D. R. *Polymer* **2009**, *50*, 6149–6156.
(28) Pfromm, P. H.; Koros, W. J. *Polymer* **1995**, *36*, 2379–2387.
(29) Dorkenoo, K. D.; Pfromm, P. H. *Macromolecules* **2000**, *33*, 3747–3751.
(30) McCaig, M. S.; Paul, D. R. *Polymer* **2000**, *41*, 629–637.
(31) Huang, Y.; Paul, D. R. *Polymer* **2004**, *45*, 8377–8393.
(32) Huang, Y.; Paul, D. R. *Macromolecules* **2006**, *39*, 1554–1559.
(33) Huang, Y.; Wang, X.; Paul, D. R. *J. Membr. Sci.* **2006**, *277*, 219–229.
(34) Roth, C. B. *Polym. Prepr.* **2009**, *50*, 792–793.
(35) Keddie, J. L.; Jones, R. A. L.; Cory, R. A. *Faraday Discuss.* **1994**, *98*, 219–230.
(36) Tsui, O. K. C.; Russell, T. P.; Hawker, C. J. *Macromolecules* **2001**, *34*, 5535–5539.
(37) Priestley, R. D.; Mundra, M. K.; Barnett, N. J.; Broadbelt, L. J.; Torkelson, J. M. *Aust. J. Chem.* **2007**, *60*, 765–771.
(38) Rittigstein, P.; Priestley, R. D.; Broadbelt, L. J.; Torkelson, J. M. *Nature Mater.* **2007**, *6*, 278–282.
(39) DeMaggio, G. B.; Frieze, W. E.; Gidley, D. W.; Zhu, M.; Hristov, H. A.; Yee, A. F. *Phys. Rev. Lett.* **1997**, *78*, 1524–1527.
(40) Kim, J. H.; Jang, J.; Zin, W. C. *Langmuir* **2001**, *17*, 2703–2710.
(41) Forrest, J. A.; Mattsson, J. *Phys. Rev. E* **2000**, *61*, R53–R56.
(42) Mattsson, J.; Forrest, J. A.; Börjesson, L. *Phys. Rev. E* **2000**, *62*, 5187–5200.
(43) Herminghaus, S.; Jacobs, K.; Seemann, R. *Eur. Phys. J. E* **2001**, *5*, 531–538.
(44) Peter, S.; Meyer, H.; Baschnagel, J.; Seemann, R. *J. Phys.: Condens. Matter* **2007**, *19*, 205119.
(45) Peter, S.; Meyer, H.; Baschnagel, J. *J. Polym. Sci., Part B: Polym. Phys.* **2006**, *44*, 2951–2967.
(46) Lipson, J. E. G.; Milner, S. T. *Eur. Phys. J. B* **2009**, *72*, 133–137.
(47) Long, D.; Lequeux, F. *Eur. Phys. J. E* **2001**, *4*, 371–387.
(48) Tsui, O. K. C.; Zhang, H. F. *Macromolecules* **2001**, *34*, 9139–9142.
(49) Ellison, C. J.; Mundra, M. K.; Torkelson, J. M. *Macromolecules* **2005**, *38*, 1767–1778.
(50) Kim, J. H.; Jang, J.; Zin, W. C. *Langmuir* **2000**, *16*, 4064–4067.
(51) Campbell, C. G.; Vogt, B. D. *Polymer* **2007**, *48*, 7169–7175.
(52) Ellison, C. J.; Ruszkowski, R. L.; Fredin, N. J.; Torkelson, J. M. *Phys. Rev. Lett.* **2004**, *92*, 095702.
(53) Riggleman, R. A.; Yoshimoto, K.; Douglas, J. F.; de Pablo, J. J. *Phys. Rev. Lett.* **2006**, *97*, 045502.
(54) Kim, S.; Mundra, M. K.; Roth, C. B.; Torkelson, J. M. *Macromolecules* **2010**, *43*, 5158–5161.
(55) Baker, E. A.; Rittigstein, P.; Torkelson, J. M.; Roth, C. B. *J. Polym. Sci., Part B: Polym. Phys.* **2009**, *47*, 2509–2519.
(56) Tompkins, H. G., Irene, E. A., Eds.; *Handbook of Ellipsometry*; Springer (William Andrew): New York, 2005.
(57) Tompkins, H. G. *A User's Guide to Ellipsometry*; Dover: New York, 1993.
(58) Donth, E. *J. Polym. Sci., Part B: Polym. Phys.* **1996**, *34*, 2881–2892.
(59) Kahle, S.; Korus, J.; Hempel, E.; Unger, R.; Höring, S.; Schröter, K.; Donth, E. *Macromolecules* **1997**, *30*, 7214–7223.
(60) Hempel, E.; Hempel, G.; Hensel, A.; Schick, C.; Donth, E. *J. Phys. Chem. B* **2000**, *104*, 2460–2466.
(61) A possible estimate for γ is 2/3, based on data by Kahle et al.[59] of the number of particles N_α per cooperatively rearranging region estimated from modulated DSC measurements of poly(*n*-butyl methacrylate-*stat*-styrene) copolymers. However, the plot suggesting $N_\alpha \sim (T_{ons} - T)^2 \sim V_\alpha \sim \xi^3$ is over a limited temperature range of only 25 K. Our data cannot be adequately fit with a value of γ near 2/3.
(62) Allowing γ or r_0 to vary did not substantially improve the fit or alter the parameters.
(63) Korus, J.; Hempel, E.; Beiner, M.; Kahle, S.; Donth, E. *Acta Polym.* **1997**, *48*, 369–378.
(64) Erwin, B. M.; Colby, R. H. *J. Non-Cryst. Solids* **2002**, *307*, 225–231.
(65) Ilton, M.; Qi, D.; Forrest, J. A. *Macromolecules* **2009**, *42*, 6851–6854.
(66) Wong, C. C.; Qin, Z.; Yang, Z. *Eur. Phys. J. E* **2008**, *25*, 291–298.
(67) The best fit parameters of $\lambda(T) = \xi(T)$ to eq 3 were $\alpha = (7.1 \pm 4.4) \times 10^{-3}$, $T_{ons} = 366 \pm 13$ K, and $r_0 = 3.4 \pm 2.0$ nm with $\gamma = 2$ fixed. We note that the errors for the $\lambda(T)$ data and the corresponding fit parameters are larger than for the $A(T)$ data and, therefore, do not assign any significant weight to their specific values other than to parametrize the data.
(68) Efremov, M. Y.; Olson, E. A.; Zhang, M.; Zhang, Z.; Allen, L. H. *Phys. Rev. Lett.* **2003**, *91*, 085703.
(69) Serghei, A.; Huth, H.; Schick, C.; Kremer, F. *Macromolecules* **2008**, *41*, 3636–3639.
(70) Serghei, A.; Kremer, F. *Macromol. Chem. Phys.* **2008**, *209*, 810–817.
(71) Efremov, M. Y.; Kiyanova, A. V.; Nealey, P. F. *Macromolecules* **2008**, *41*, 5978–5980.
(72) Erber, M.; Tress, M.; Mapesa, E. U.; Serghei, A.; Eichhorn, K.-J.; Voit, B.; Kremer, F. *Macromolecules* **2010**, ASAP DOI: 10.1021/ma100912r.
(73) Huth, H.; Minakov, A. A.; Schick, C. *J. Polym. Sci., Part B: Polym. Phys.* **2006**, *44*, 2996–3005.
(74) Lu, H.; Chen, W.; Russell, T. P. *Macromolecules* **2009**, *42*, 9111–9117.
(75) Mundra, M. K.; Ellison, C. J.; Behling, R. E.; Torkelson, J. M. *Polymer* **2006**, *47*, 7747–7759.
(76) Fakhraai, Z.; Sharp, J. S.; Forrest, J. A. *J. Polym. Sci., Part B: Polym. Phys.* **2004**, *42*, 4503–4507.
(77) Raegen, A. N.; Massa, M. V.; Forrest, J. A.; Dalnoki-Veress, K. *Eur. Phys. J. E* **2008**, *27*, 375–377.

(78) Prucker, O.; Christian, S.; Bock, H.; Ruhe, J.; Frank, C. W.; Knoll, W. *Macromol. Chem. Phys.* **1998**, *199*, 1435–1444.
(79) Fakhraai, Z.; Valadkhan, S.; Forrest, J. A. *Eur. Phys. J. E* **2005**, *18*, 143–148.
(80) Fakhraai, Z.; Forrest, J. A. *Phys. Rev. Lett.* **2005**, *95*, 025701.
(81) Kawana, S.; Jones, R. A. L. *Phys. Rev. E* **2001**, *63*, 021501.
(82) Peter, S.; Napolitano, S.; Meyer, H.; Wubbenhorst, M.; Baschnagel, J. *Macromolecules* **2008**, *41*, 7729–7743.
(83) Roth, C. B.; Pound, A.; Kamp, S. W.; Murray, C. A.; Dutcher, J. R. *Eur. Phys. J. E* **2006**, *20*, 441–448.
(84) Grohens, Y.; Hamon, L.; Reiter, G.; Soldera, A.; Holl, Y. *Eur. Phys. J. E* **2002**, *8*, 217–224.
(85) Yang, Z.; Fujii, Y.; Lee, F. K.; Lam, C.-H.; Tsui, O. K. C. *Science* **2010**, *328*, 1676–1679.
(86) Pryamitsyn, V.; Ganesan, V. *Macromolecules* **2010**, *43*, 5851–5862.